Bragg Scatter Detection by the WSR-88D. Part II: Assessment of Z_{DR} Bias Estimation

LINDSEY M. RICHARDSON

Radar Operations Center, National Weather Service, and Centuria Corporation, Norman, Oklahoma

W. DAVID ZITTEL AND ROBERT R. LEE

Radar Operations Center, National Weather Service, Norman, Oklahoma

VALERY M. MELNIKOV

Cooperative Institute for Mesoscale Meteorological Studies, University of Oklahoma, and National Severe Storms Laboratory, Norman, Oklahoma

RICHARD L. ICE

Radar Operations Center, National Weather Service, Norman, Oklahoma, and 557th Weather Wing, Offutt Air Force Base, Nebraska

JEFFREY G. CUNNINGHAM

557th Weather Wing, Offutt Air Force Base, Nebraska

ABSTRACT

Clear-air Bragg scatter (CABS) is a refractivity gradient return generated by turbulent eddies that operational Weather Surveillance Radar-1988 Doppler (WSR-88D) systems can detect. The randomly oriented nature of the eddies results in a differential reflectivity (Z_{DR}) value near 0 dB, and thus CABS can be used as an assessment of Z_{DR} calibration in the absence of excessive contamination from precipitation or biota. An automated algorithm to estimate Z_{DR} bias from CABS was developed by the Radar Operations Center and can be used to assess the calibration quality of the dual-polarized WSR-88D fleet. This technique supplements existing Z_{DR} bias assessment tools, especially the use of other external targets, such as light rain and dry snow.

The estimates of Z_{DR} bias from CABS using a 1700–1900 UTC time window were compared to estimates from the light rain and dry snow methods. Output from the automated CABS algorithm had approximately the same amount of bias reported as the light rain and dry snow estimates (within ±0.1 dB). As the 1700–1900 UTC time window appeared too restrictive, a modified version of the algorithm was tested to detect CABS diurnally on a volume-by-volume basis (continuous monitoring). Continuous monitoring resulted in a two- to fourfold increase in the number of days with CABS detections. Results suggest estimates from CABS are viable for many sites throughout the year and provide an important addition to existing bias estimation techniques.

1. Introduction

The dual-polarization Weather Surveillance Radar-1988 Doppler (WSR-88D) systems produce a differential reflectivity field (Z_{DR}) that is used for visual analysis and as input for derived products. This field can be impacted by variations of individual hardware components in a WSR-88D. A ZDR_{Offset}, computed from an engineering-derived method, is applied automatically to the measured Z_{DR} field to account for biases introduced by normal hardware component variations (Melnikov et al. 2013; Cunningham et al. 2013; Ice et al. 2014). If the ZDR_{Offset} fails to correctly capture some aspect of hardware bias, the result is a bias in the Z_{DR} field. Thus, an error in ZDR_{Offset} translates to a Z_{DR} bias.

Corresponding author e-mail: Lindsey M. Richardson, lindsey.m.richardson@noaa.gov

TABLE 1. Descriptions of the datasets used in this study.

Datasets			
Name	Description	Method	Time frame
Set A	155 sites for 1 year	2-h time window	Oct 2013–Sep 2014
Set B	17 sites for 4 months	Continuous monitoring	Oct 2013; Jan, Apr, Jul 2014
Set C	155 sites for 1 month	Continuous monitoring	Apr 2014

The Z_{DR} bias impairs visual interpretation and negatively impacts radar-derived products, especially quantitative precipitation estimation (QPE) products. Previous research determined that accuracy in the measured Z_{DR} bias of ±0.2 dB is desirable, especially to mitigate errors in rain rates calculated with Z–Z_{DR} relationships (e.g., Bringi and Chandrasekar 2001; Ryzhkov et al. 2005). Gorgucci et al. (1999) proposed a method of calibrating Z_{DR} bias in light rain by vertically pointing the radar antenna, but this is not possible on a WSR-88D due to hardware constraints. Also, the lack of suitable precipitation returns throughout the year across the United States necessitates other estimation techniques.

The engineering-derived method originally developed to calibrate Z_{DR} on the WSR-88D has proven challenging to use (Ice et al. 2013, 2014). Instead, external target methods monitoring light rain and dry snow were developed from operational data scans (where elevation angles go up to only 19.5°). These external target methods focus on conditions with expected intrinsic Z_{DR} values (Cunningham et al. 2013; Zittel et al. 2014). Comparing the Z_{DR} from the radar data to the intrinsic value ($ZDR_{Intrinsic}$) gives an assessment of Z_{DR} bias. To complement the existing rain and snow methods, the Radar Operations Center (ROC) developed an algorithm to use returns from clear-air Bragg scatter (CABS) for finding Z_{DR} bias estimates on any dual-polarization WSR-88D. Described in detail in Richardson et al. (2017, hereinafter Part I), the algorithm uses the following steps to calculate an estimate for Z_{DR} bias:

1) Use volume coverage pattern (VCP) limits (only VCPs 32 and 21), range limits (10–80 km), and elevation angle limits (~2.4°–4.5°) to avoid contamination from ground clutter and precipitation. Initial testing focused on specified 2-h time frames (1700–1900 and 0000–0200 UTC).
2) Accumulate all Z range gates within the spatial limits into a histogram over the time window.
3) Apply base data filters (filters based on reflectivity, signal-to-noise ratio, correlation coefficient, velocity, and spectrum width) to isolate radar range gates associated with CABS. The Z_{DR} values from range gates that pass are accumulated into a histogram over the time window.

4) Apply statistical filters (range gate count $\geq 10\,000$ and interquartile range < 0.9 dB) applied to the Z_{DR} histogram to ensure adequate samples for statistics and test for excessive contamination, respectively.
5) A precipitation filter based on the Z histogram (90th percentile of reflectivity (Z90th) ≤ -3.0 dBZ) further tests for precipitation contamination.
6) If the statistical and precipitation filters are passed, then the mode of the Z_{DR} histogram gives an estimate of the Z_{DR} bias.

These filters were specifically chosen to help isolate radar range gates with CABS returns that could potentially be useful for Z_{DR} bias estimation.

To assess the applicability and availability of automated Z_{DR} bias estimates from CABS, several datasets were investigated (Table 1). Set A consists of the automated 1700–1900 UTC CABS Z_{DR} bias estimates for October 2013 through September 2014 from 155 WSR-88D sites. Set B consists of continuous monitoring (section 2c) estimates from 17 sites for October 2013, January 2014, April 2014, and July 2014. Set C consists of continuous monitoring estimates from 155 sites for April 2014. Operational Level II[1] data were processed using an offline MATLAB routine for radars across the contiguous United States (CONUS) and outside-CONUS (OCONUS) sites in Alaska, Hawaii, and Puerto Rico. A map of all sites included is shown in Fig. 1. As some sites have two separate transmitters (channel 1 and channel 2), the information is separated by channel; each channel can have a unique Z_{DR} bias. Dual-channel sites are displayed as stacked boxes on the map.

Section 2 explores how Z_{DR} bias estimates from the automated CABS routine compare with the existing rain and snow methods. Section 3 compares the seasonal, spatial, and temporal availability of Z_{DR} bias estimates from CABS from the original algorithm in the 1700–1900 UTC window (2-h version) to a modified continuous monitoring version of the algorithm. Section 4 concludes with a summary and discussion.

---

[1] See Crum et al. (1993) for the distinction between the various levels of radar data available.
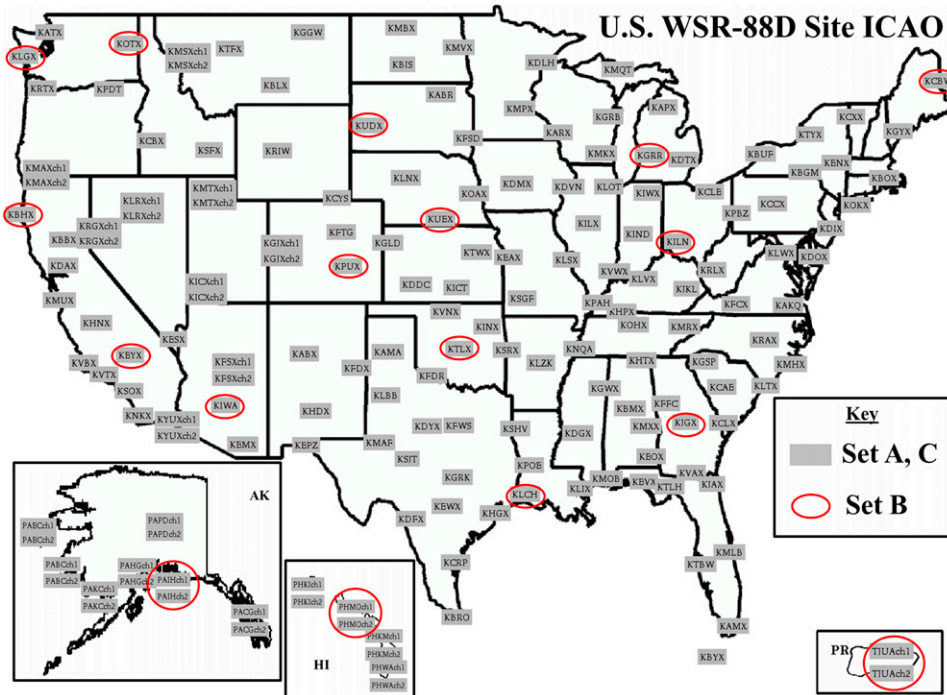
FIG. 1. Map of CONUS and OCONUS WSR-88Ds considered in this study as identified by their International Civil Aviation Organization (ICAO) code. The locations of the set B sites are listed in Table 2.

2. Z_{DR} bias estimation from external targets

a. Light rain and dry snow overview

To assess the Z_{DR} bias from an operational system that cannot point vertically due to hardware constraints, and is undesirable from operational time constraints, the use of external hydrometeor targets was proposed. Specifically, rain and snow data from elevation scans within operational WSR-88D VCPs were explored. These independent hydrometeor estimates are sufficiently separate to use as an assessment of Z_{DR} bias (and to determine ZDR$_{Offset}$ error). Cunningham et al. (2013) and Zittel et al. (2014) discuss these methods in detail. A brief summary is presented here to facilitate comparison to the automated CABS algorithm.

The light rain method looks for reflectivity (Z) range gates around 20–30 dBZ to estimate Z_{DR} bias. On the WSR-88D, light rain between 20 and 30 dBZ (within certain rain regimes) generally has ZDR$_{Intrinsic}$ values from 0.23 to 0.55 dB (Schuur et al. 2001, 2005; Zhang et al. 2006). All of the rain range gates must be well below the radar-estimated melting layer (at least 1 km). Estimates are taken by grouping data from 3–6-h time periods related to the radar returns. A major caveat to the light rain method comes from the large range of possible particle sizes in a radar range gate (or

resolution volume). Light rain events could contain larger drops that bias the Z_{DR} estimate high. Additionally, the intrinsic values used in the method are based on a dataset limited to a narrow region in the central United States. This could introduce estimation error based on distribution differences related to rain/storm type or geographic region.

The second hydrometeor method uses dry snow, focusing on dry aggregates above the WSR-88D radar-estimated melting layer, to estimate a Z_{DR} bias. Zittel et al. (2014) use 0.2 dB as the $Z_{DR\_Intrinsic}$ value of dry snow for their algorithm, as suggested by empirical evidence (Meischner et al. 1991; Vivekanandan et al. 1994). The same value is used throughout this study. Similar to the light rain method, estimates are made by grouping data from 3–6-h time periods dynamically related to the actual radar returns. Only range gates classified as "dry snow" by the WSR-88D hydrometeor classification algorithm are considered for analysis. Ice aggregates generally have low bulk densities and certain shapes that give them a slightly positive intrinsic Z_{DR}. Variations in the shapes and bulk densities lead to deviations from the frequent ZDR$_{Intrinsic}$ value of 0.2 dB from aggregates (Meischner et al. 1991; Vivekanandan et al. 1994; Straka et al. 2000). These variations in the intrinsic Z_{DR} can lead to small errors in the estimation of
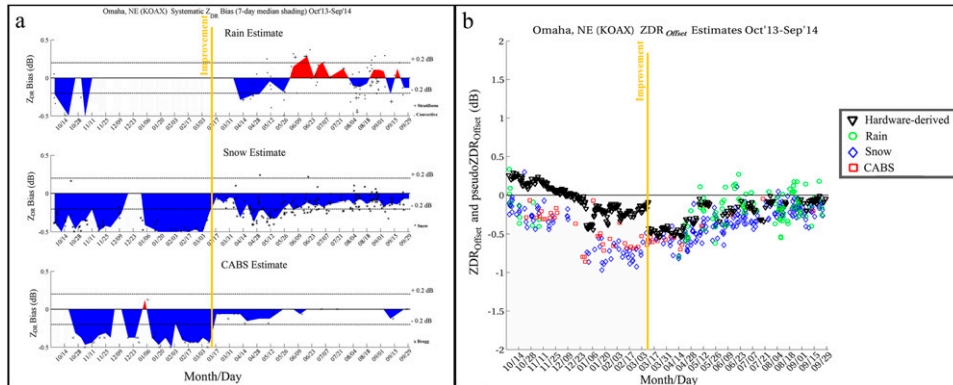
FIG. 2. (a) Shade chart from Omaha, NE (KOAX) showing Z_{DR} bias estimates (scatter points) from (top) light rain, (middle) dry snow, and (bottom) CABS. The dashed lines are ±0.2 dB, and the 7-day median of the scatter points creates the shading. The yellow "improvement" line denotes where maintenance occurred; estimates came closer to −0.2 dB overall after the maintenance compared to −0.5 dB prior. (b) Hardware-derived ZDR_{Offset} vs the pseudoZDR$_{Offset}$ from external targets. After the improvement line, the ZDR_{Offset} values are much closer to the external target estimates that match the lower Z_{DR} bias, as seen in the shade chart.

Z_{DR} bias. Furthermore, the WSR-88D radar-estimated melting layer or hydrometeor classification could be in error and cause discrepancies in the types of returns used to make a Z_{DR} bias estimate. These cumulative errors are relatively small (less than a 0.1 dB) over a long time span for the dry snow method in most cases. An obvious limitation of both the rain and snow techniques is their reliance on suitable meteorological conditions.

b. Calculation of Z_{DR} bias

Using the Z_{DR} estimates from the automated CABS routine can supplement the existing rain and snow methods to distinguish whether a radar site has a Z_{DR} bias. It is an example of Z_{DR} bias estimation in periods of clear weather. Bragg scatter at S-band frequencies is caused by turbulent vortices of about 5 cm in size. Typically, the strongest Bragg scatter occurs at the top of boundary layers, where turbulence is well developed and vortices are randomly oriented. While the rain and snow methods can introduce errors from incorrectly approximated ZDR$_{Intrinsic}$ values, the random orientation of CABS gives ZDR$_{Intrinsic}$ of 0 dB and avoids such additional error.

As the light rain, dry snow, and CABS methods are independent and based on different types of returns, each one can give a certain degree of confidence in an existing Z_{DR} bias. On the WSR-88D, Z_{DR} is calculated as

$$Z_{DR} = ZDR_{Measured} - ZDR_{Offset}, \qquad (1)$$

where the ZDR$_{Offset}$ attempts to handle a suite of possible hardware-related biases (Cunningham et al. 2013; Ice et al. 2014). If Z_{DR} bias is calculated such that

$$Z_{DR} \text{bias} = Z_{DR} - ZDR_{Intrinsic}, \qquad (2)$$

then a pseudoZDR$_{Offset}$, which is the ZDR$_{Offset}$ added to the Z_{DR} bias, gives an estimate of how much the measured Z_{DR} differs from the intrinsic Z_{DR}, written as

$$\begin{aligned} \text{pseudoZDR}_{Offset} &= Z_{DR}\text{bias} + ZDR_{Offset} \\ &= ZDR_{Measured} - ZDR_{Intrinsic}. \end{aligned} \quad (3)$$

Thus, errors in the offset correction value appear as a Z_{DR} bias in the radar data. Tracking the estimated Z_{DR} bias and the pseudoZDR$_{Offset}$ from the three methods can confirm existing calibration bias at a radar site if the trend is seen over a sufficient amount of time (e.g., 1 month).

c. CABS versus other methods

To display trends in Z_{DR} bias over long time periods (months up to a year), shade charts are a convenient tool. The vertically stacked shade charts (example in Fig. 2a) shows the individual Z_{DR} estimates (scatter points) from light rain (top), dry snow (middle), and CABS (bottom). While CABS has only one estimate per day from the 1700–1900 UTC time frame, the light rain and dry snow methods may have multiple estimates per day. Estimates from each method are grouped into distinct 7-day periods and a median value sets the shading threshold. Red colors indicate positive (above 0.0 dB) bias, while blue colors indicate negative (below 0.0 dB) bias. The dashed horizontal lines portray recommended threshold limits of ±0.2 dB following Ryzhkov et al. (2005), Bechini et al. (2008), Cunningham et al. (2013),
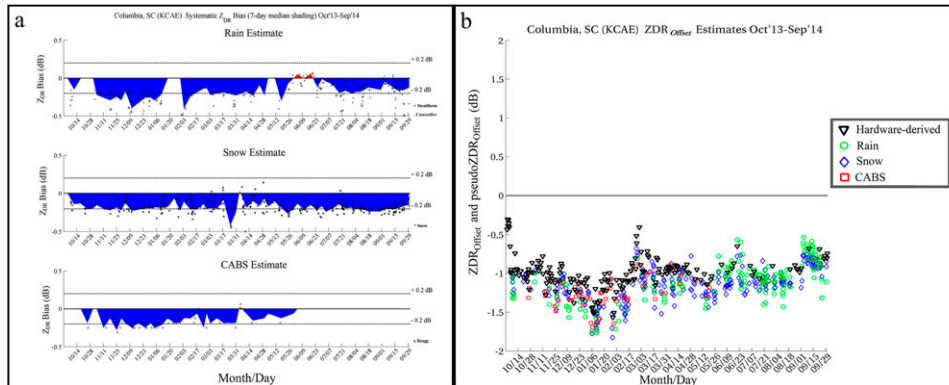
FIG. 3. As in Fig. 2, but for Columbia, SC (KCAE). This site had a consistent slightly negative Z_{DR} bias for the entire time frame according to the shading trend. The lack of CABS from June 2014 to September 2014 could be due to seasonal availability of Bragg scatter or widespread contamination from biota or precipitation during this time of year.

and Zittel et al. (2014). Radars with consistent shading, not just single events, beyond the ± 0.2-dB limit over time are considered to have a Z_{DR} bias that would adversely impact QPE and other products. In general, excluding hardware failures, the Z_{DR} bias value at a site is relatively constant (within ± 0.2 dB of a value) over several months or longer, such as seen in Figs. 2a, 3a.

Shade charts were created for each site/channel and were visually inspected for the estimated Z_{DR} bias and trends between light rain, dry snow, and CABS. Overall, the three methods reveal similar estimates of Z_{DR} bias when methods are available in the same time frame; the method estimates are generally within ± 0.2 dB of each other. For example, from October 2013 to March 2014, all three methods agree that the Z_{DR} bias at Omaha, Nebraska (KOAX), is between -0.4 and -0.5 dB. Maintenance occurred in early March, and all three methods show an improvement, as the overall shading trend is closer to -0.2 dB through September (Z_{DR} bias moved closer to 0 dB). Higher values in the rain method compared to CABS and snow suggests contamination from larger drops in these estimates. The CABS estimates agree with the snow estimates throughout the year on the relative value of Z_{DR} bias at this site. One CABS case appears to be contaminated, as it shows a positive bias estimate within the negative trend (near the beginning of January 2014).

Another way of viewing the Z_{DR} bias is to plot pseudoZDR$_{Offset}$ values for each external target method and compare those values to the hardware-derived ZDR$_{Offset}$. Because the hardware-derived ZDR$_{Offset}$ was removed from the measured Z_{DR} to find the total Z_{DR}, we can add it back into the Z_{DR} bias estimates, which should be near zero from an unbiased site (Fig. 2b). Unlike Z_{DR} bias, ZDR$_{Offset}$ (and pseudoZDR$_{Offset}$)

values are not expected to be near zero or fall within a certain tolerance limit at an unbiased site. When the values of hardware-derived ZDR$_{Offset}$ (black triangles) do not align with the pseudoZDR$_{Offset}$ estimates from the external targets (uniquely coded by shape and color), the system has a bias as depicted in the associated shade chart.[2] Thus, as the Z_{DR} bias is reduced in magnitude after March 2014 (reflected with the shading values moving from -0.4 to -0.2 dB), the pseudoZDR$_{Offset}$ and ZDR$_{Offset}$ are comparable.

Figure 3 shows a shade and ZDR$_{Offset}$ chart from Columbia, South Carolina (KCAE), in the same format as Fig. 2. This example shows how a site's Z_{DR} bias is relatively stable over a long period of time without hardware failures or maintenance actions performed. All three methods show a bias near -0.2 dB for the entire year. We do not expect the individual estimates (scatter points) to be equivalent due to differences in estimation techniques. From June through September 2014, there is a distinct lack of CABS estimates at this site. This may be unexpected from a site with ample moisture such as KCAE, yet the automated CABS algorithm may not be passing cases due to biota or precipitation contamination in the warmer months. Limitations from seasonal variability are explored further in section 3.

Instead of comparing individual estimates for exact similarity, as they are separated by time and other parameters, relative closeness can be assessed by grouping data over a longer time frame. Figure 4 shows the

---

[2] The other shapes' values minus the triangles' values (external minus internal) are equivalent to the Z_{DR} bias seen in the shade chart.
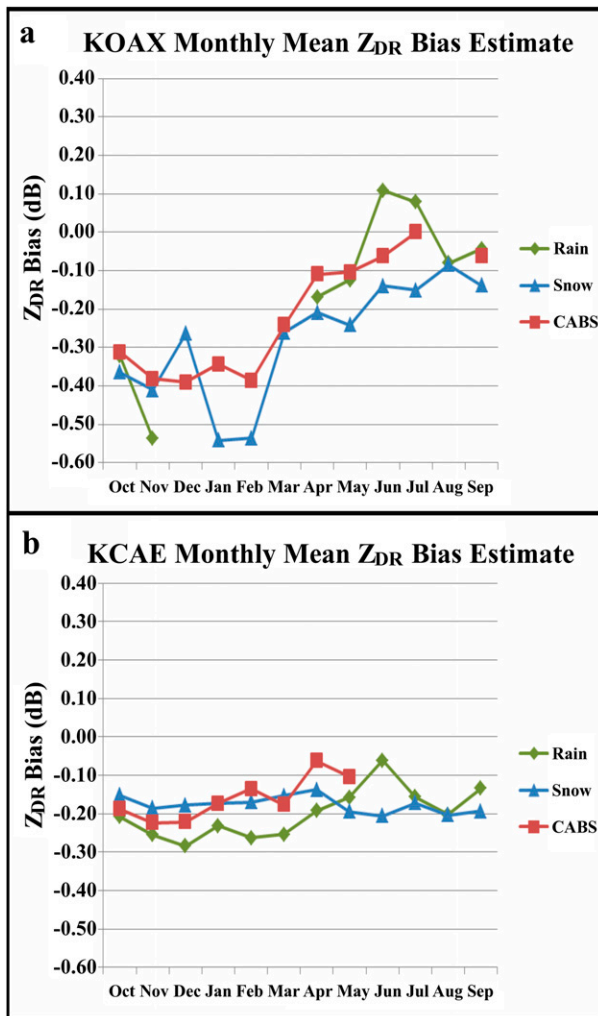
FIG. 4. The mean Z_{DR} bias estimate over an entire month from October 2013 to September 2014 from rain, snow, and CABS (2-h version) for (a) Omaha, NE (KOAX) and (b) Columbia, SC (KCAE). Missing data cause disconnected lines. The three methods are generally within ±0.1 dB of each other at a given site.

monthly mean Z_{DR} bias estimate from the three methods from KOAX and KCAE using the scatter points in the shade charts. Even with the caveats of each individual method, the monthly estimates are generally within 0.1 dB of each other. The larger variability and the difference of the light rain estimates at KOAX very likely come from contamination of larger drops. Perhaps our specific setup of external target estimation cannot be more accurate than 0.2 dB, but a discussion of the full extent of variability from these three methods is beyond the scope of this paper and should be addressed in future studies. In particular, the same type of measuring metric for all three external target estimates is recommended (e.g., a daily median) instead of the very different measurements used in this paper. Information on the

availability of CABS should precede certain statistical analysis, as the potential for reduced availability throughout the year at certain locations can skew statistical tests. In general, CABS-based Z_{DR} bias estimates and trends in those biases match with the precipitation-based independent verification data, but the question of CABS availability still remains.

3. Availability of CABS estimates

a. Overview

Part I describes the setup of an automated routine that uses specific base data filters, statistical filters, range restrictions, elevation angle restrictions, VCP restrictions, and temporal restrictions to automatically assess Z_{DR} bias from CABS returns in operational WSR-88D radar data. Though the 1700–1900 UTC time window highlights estimation in the central plains, it should correspond to a time of day with sufficient diurnal heating to generate CABS related to boundary layer dynamics for most CONUS radar sites. However, temporal restrictions could be a major limiting factor at finding Z_{DR} bias estimates from CABS in certain geographical regions in certain times of the year. For example, in Columbia (Fig. 3), CABS estimates are available along with light rain and dry snow estimates for a majority of the year until the warmer months. This could be from the temporal restriction and/or contamination in that location. As previous Bragg scatter studies were confined to limited geographic regions, we explore the availability of estimates from our automated routine across the United States over a 1-yr time frame.

To further assess the impact of a temporal restriction, datasets were investigated using both the 1700–1900 UTC time window and a continuous monitoring version of the algorithm modified slightly. For this paper, we focus on October 2013, January 2014, April 2014, and July 2014 data to assess seasonal variability. Zittel et al. (2015) further describe general information on availability in other months and information about the light rain and dry snow data.

b. 1700–1900 UTC availability

Estimates of Z_{DR} bias from CABS were automatically calculated from the mode of data passing base data, statistical, and precipitation filters between 1700 and 1900 UTC in the original time-restricted version. With a chance for one estimate per day from CABS, the number of days with CABS estimates was counted per month for each site as a metric of frequency. Figure 5 shows the count of CABS estimates for the four focus months using the 1700–1900 UTC dataset for 155 radars (set A).
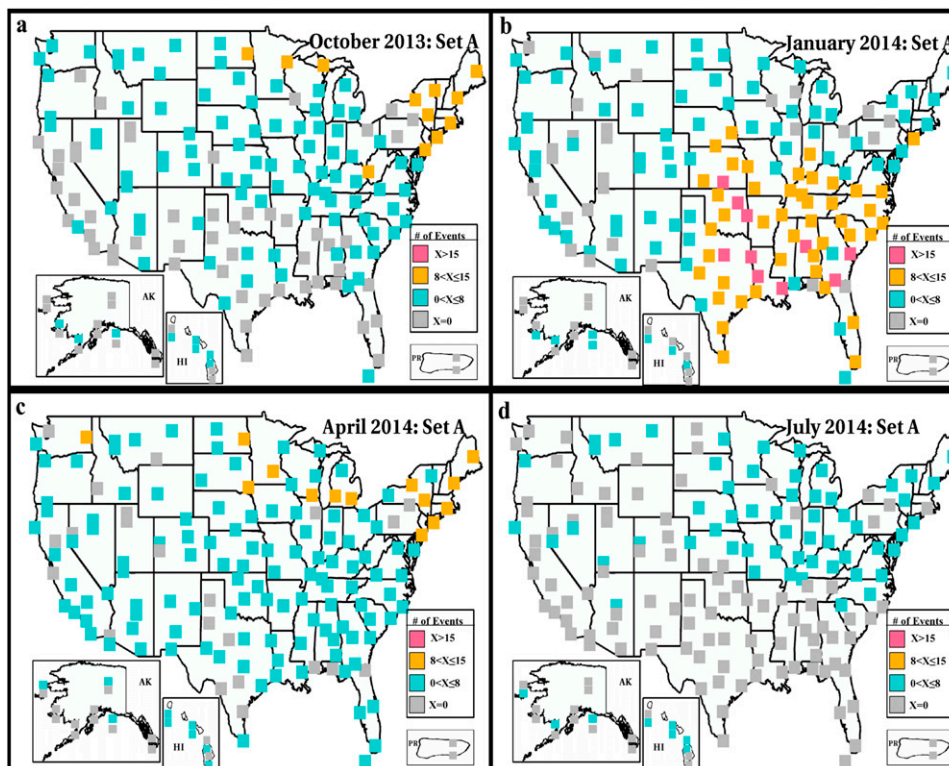
Fig. 5. Number of CABS cases per site/channel for (a) October 2013, (b) January 2014, (c) April 2014, and (d) July 2014 from set A. The color steps from bottom to top represent 0 events (gray), 1–8 events (blue), 9–15 events (yellow), and greater than 15 events (pink). VCP selection, precipitation coverage, and biota coverage impact the number of days with CABS detections in various seasons.

Color-coded frequency categories are broken out as follows: 0 events (gray), 1–8 events (blue), 9–15 events (yellow), and greater than 15 events (pink; over half of a month).

Many sites have CABS estimates throughout the year during this 2-h time window. July 2014 is a striking exception, showing the lack of CABS across much of the CONUS despite the typically more humid environment. Conversely, January 2014 portrays the greatest availability of CABS estimates despite generally drier and cooler conditions. This seasonal difference, most prevalent in southern portions of the CONUS, is largely due to biota and precipitation contamination preventing estimation of Z_{DR} bias from CABS in the warmer months. Biota can sharply skew Z_{DR} bias estimates far away from 0 and thus are undesirable returns even if a Bragg scattering layer is present. We surmise that in January, there is just enough moisture and surface heating without contamination from biota to allow Bragg scatter to be detected much of the time. Studies suggest the insects are not as prevalent in April, as they have not yet hatched/grown/thawed but as adults they linger into October before overwintering (e.g., Tauber et al. 1986).

Additionally, an increase in the frequency of convection and the North American monsoon in the west contribute to sites using precipitation-oriented VCPs in the warmer months (Adams and Comrie 1997; SPC 2013).

It has been shown that marine and continental Bragg scattering layers can have different characteristics in terms of thickness and amount of moisture (Melnikov et al. 2011, 2013; Davison et al. 2013a,b). However, the algorithm appears to show no preference to coastal, plain, or desert locations regarding the availability of estimates as shown in Fig. 5. San Juan, Puerto Rico (TJUA), presents a unique exception with no CABS estimates for any month during the 1700–1900 UTC time frame. VCP selection and/or contamination are likely preventing CABS estimates at this location during this time frame.

The 1700–1900 UTC time frame itself limits the potential for estimation, as CABS occurs more often than in this limited span of time. Removing the temporal restriction could bolster the amount of estimations from sites throughout the year, including places such as KCAE during the warmer months (Fig. 3 showed no CABS estimates in warmer months).

c. Continuous monitoring availability

Slight modifications were made to remove the temporal limitation for estimating Z_{DR} bias from CABS. Continuous monitoring for CABS attempts to estimate Z_{DR} bias in each volume scan. For reference, a typical WSR-88D volume scan completes in 5–10 min. The base data filters, range/elevation angle limits, and allowed VCPs remain the same. The Z_{DR} values from range gates that pass the filters are placed into a histogram of 0.0625-dB class intervals. The Z values from the range, elevation angle, and VCP limits are placed in a separate histogram for each volume scan as well. Preliminary analysis of CABS cases with little to no contamination had generally at least 600 range gates passing the filter set per volume scan, so a 600 range gate count requirement must be passed before an estimate is made. If all of the tests are passed, including the precipitation filter based on the Z histogram on the volume scan, a mode of the corresponding Z_{DR} histogram is calculated. Because 600 range gates is a relatively small sample size, the volume-by-volume estimates can be noisy.

To remove the volume-by-volume noisiness of the modes, a moving average of the volume-by-volume Z_{DR} modes is calculated from the 12 most recent volume scans. This average is calculated only if the sum of passing Z_{DR} range gates from the 12-volume set is ≥10 000 range gates. Furthermore, only Z_{DR} modes from passing volume scans (that pass the statistical and precipitation filters) are included in the moving 12-volume average calculation (12-volume average). Data from volume scans in a nonallowed VCP are ignored. For example, if the most recent volume scan is in a nonallowed VCP, then the data are ignored and the 12-volume average effectively uses only 11 volumes of data. This behavior mimics use on an operational WSR-88D system.

Data from the four focus months were investigated to compare with data in Fig. 5 (October 2013, January 2014, April 2014, and July 2014). We assessed data from 17 sites (listed in Table 2 and circled in Fig. 1) selected from more arid to more moist regions roughly based on the Köppen–Geiger climatology map (Peel et al. 2007). This 4-month dataset of 17 sites constitutes set B. Instead of comparing how many total estimates are found on a single day, the number of days with at least one CABS estimate is counted to compare with set A.

The fraction of a month with CABS estimates from the four focus months is compared for set A and set B from the 17 sites (Fig. 6). Continuous monitoring on average shows a twofold to fourfold increase in the number of days with Z_{DR} bias estimates from CABS. This is especially true at TJUA, with no estimates in the

TABLE 2. List of the sites used for set B continuous monitoring tests.

WSR-88D site ICAO	Location (city, state)
KIWA	Phoenix, AZ
KOTX	Spokane, WA
KEYX	Edwards Air Force Base, CA
KUDX	Rapid City, SD
KPUX	Pueblo, CO
KUEX	Hastings, NE
KTLX	Oklahoma City, OK
KILN	Cincinnati, OH
KJGX	Robbins AFB, GA
KGRR	Grand Rapids, MI
KBHX	Eureka, CA
KLCH	Lake Charles, LA
KCBW	Caribou, ME
KLGX	Langley Hill, WA
PAIH	Middleton Island, AK
PHMO	Molokai, HI
TJUA	San Juan, PR

1700–1900 UTC time window and almost half of the month with estimates on average when using continuous monitoring. Most sites follow the trend seen in Fig. 5: there are generally more CABS estimates in cooler months than in warmer months. Increased biota coverage and increased convective precipitation (for which sites would select a more precipitation-oriented VCP) are likely the biggest factors limiting CABS estimates with the algorithm regardless of time limitations.

Table 3 shows the average VCP usage from the 4 months for set A and set B. Even with the large difference in the total number of sites, sites use an allowed VCP (21 or 32) over half of the time throughout the year. Thus, sites have the potential to estimate Z_{DR} bias from CABS based on VCP selection a large portion of the time. The relatively high percentage of July 2014 data in the not available (N/A) category in set B is due to internal data feed errors and does not reflect radar downtime. Increased convective precipitation coverage affects VCP selection during the warmer months—sites select more convection-oriented VCPs.

A subset of four sites shows seasonal and diurnal variability in more detail in Fig. 7. The number of continuous monitoring CABS estimates, separated by hour, is displayed for each focus month. Approximate times for sunrise and sunset are imposed on the charts in dashed and solid lines respectively. Because CABS is most commonly related to refractivity gradients (e.g., Atlas 1959; Ottersten 1969; Part I), it is unsurprising to see arid regions having fewer estimates than coastal sites with more moisture. Phoenix, Arizona (KIWA), has many fewer estimates than the other three sites shown due to its arid environment. Interestingly, the bulk of
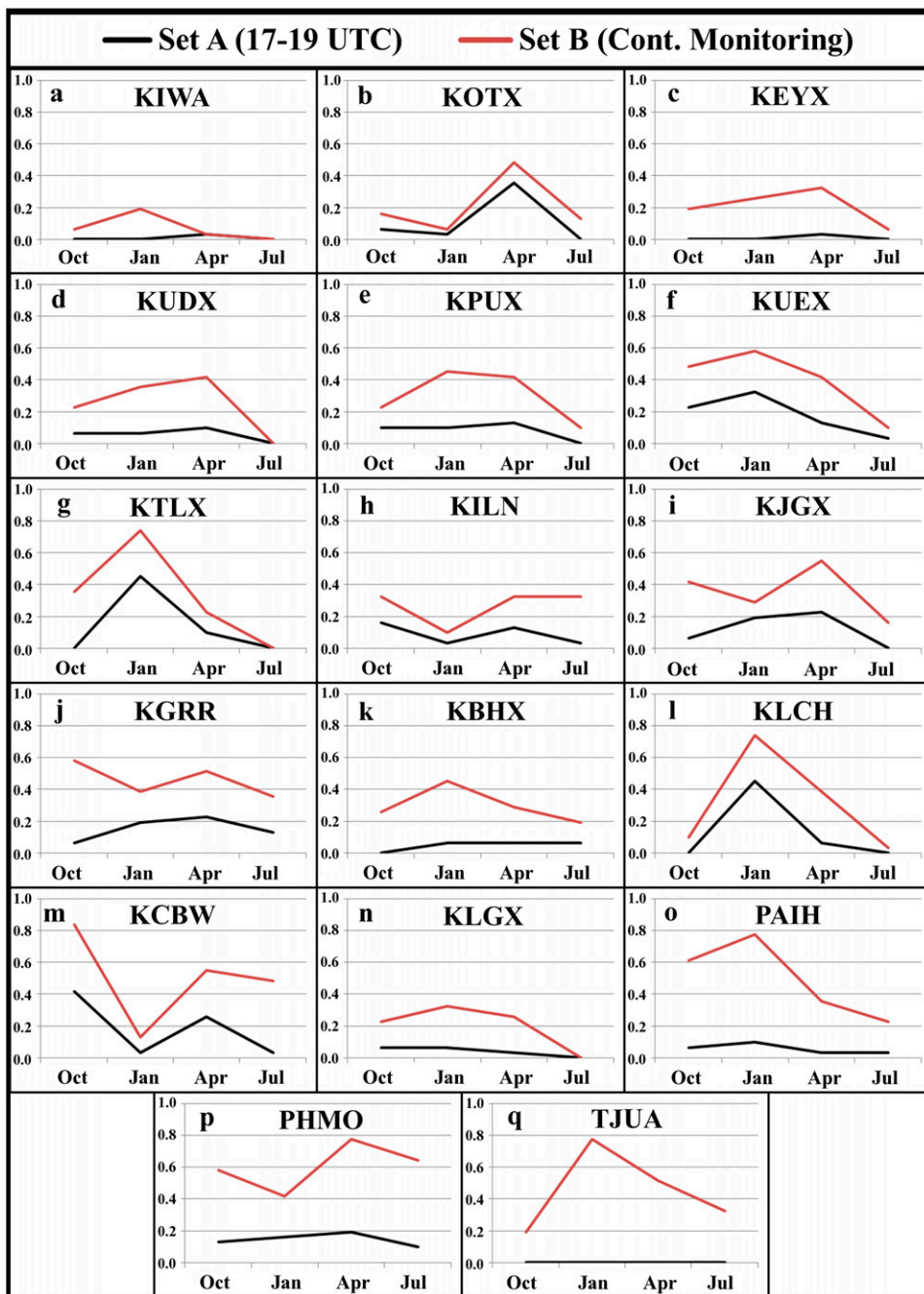
FIG. 6. The fraction of each month CABS is available from set A (black) and set B (red) for the 17 climatologically diverse sites for the four focus months. Location names are specified in Table 2. Continuous monitoring often gives 2–4 times as many days with CABS estimates.

CABS estimates at KIWA come near sunrise, when mixing first starts. We surmise that higher relative humidity from evaporating dew and cooler temperatures just before sunrise are contributing to refractivity gradients strong enough for detection by radar. The overnight availability in January may be from moisture influx

from the northwest, common during the winter months. The afternoon peak at Hasting, Nebraska (KUEX), corresponds well with the original plains-centric algorithm. As such, most CABS at this site is likely linked to convective boundary layer dynamics. Coastal locations such as Middleton Island, Alaska (PAIH), and TJUA

TABLE 3. Percentage of total volume scans from sets A and B that were in an allowed CABS routine VCP (32 or 21), a non-allowed VCP (Other), or not available (N/A). Columns may not sum to 100% due to rounding.

| | (i) Percent of VCP usage from set A | | | |
VCP	Oct 2013	Jan 2014	Apr 2014	Jul 2014
32/21	66.4	69.4	61.8	61.5
Other	30.5	25.9	34.3	34.5
N/A	3.2	4.7	3.9	4.0
	(ii) Percent of VCP usage from set B			
VCP	Oct 2013	Jan 2014	Apr 2014	Jul 2014
32/21	73.9	74.9	66.7	33.6
Other	24.6	24.3	25.3	40.3
N/A	1.6	0.8	8.0	26.1

appear to have no diurnal preference due to the constant availability of moisture. However, TJUA shows a unique lack of CABS during the 1300–1500 LST (1700–1900 UTC) time window corresponding with isolated precipitation forming, resulting in a change in VCP and/or decreased chances of passing the precipitation filter.

For assessing the equivalency of the Z_{DR} bias between the 2-h and continuous monitoring versions, the monthly mean of Z_{DR} bias was calculated for both methods.

Results from the 17 sites are shown in Table 4 with a subset plotted in Fig. 8. Recall that each site/channel can have a unique Z_{DR} bias and that some channels are not used very often. The monthly means of Z_{DR} bias from continuous monitoring agree quite well with the 2-h means, mostly within 0.1 dB. This gives confidence that an increased amount of estimates, even with a potential for increased variability and contamination, can give reasonably accurate estimations of Z_{DR} bias when using a sufficient time frame of data (such as a month). Additionally, the specific setup of base data filters, statistical filters, range limitations, and elevation angle limitations used in the routines works well enough to give a reliable Z_{DR} bias estimate based on CABS over a longer time frame. As the mean is a nonresistant statistic, it can be impacted by the total number of estimates with potential for random error. We suspect this contributes to the more than 0.1-dB difference between the means at Pueblo, Colorado (KPUX), in October.

To further assess the spatial availability with continuous monitoring, April 2014 data were evaluated for the 155-site set (set C). Figure 9 reveals that many sites have CABS estimates for almost half of the month—55 sites exceed 15 days with estimates compared to set A, which
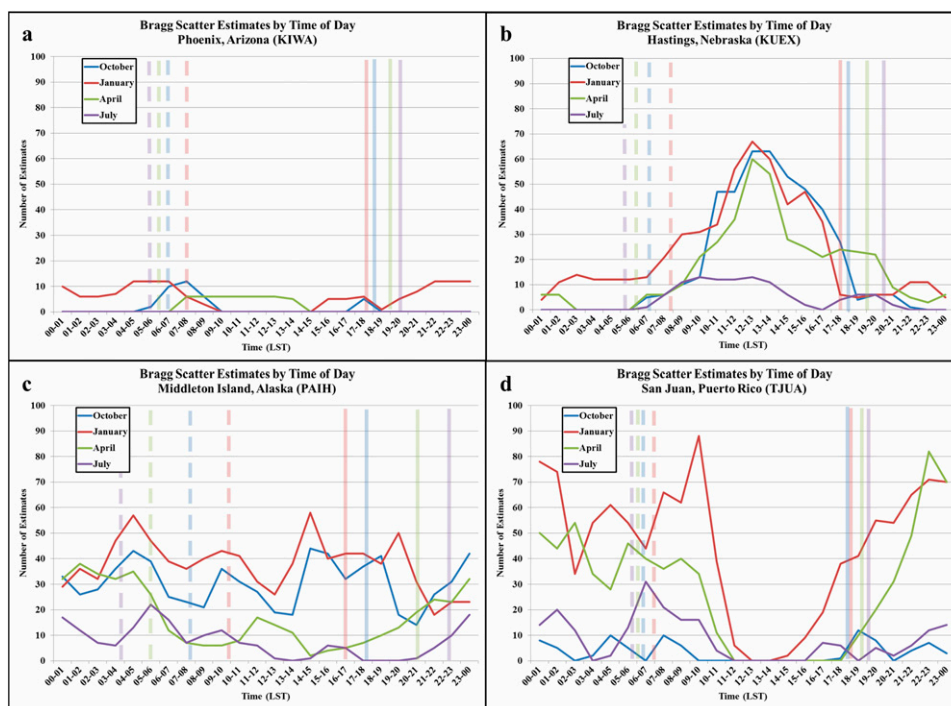

FIG. 7. Number of continuous monitoring CABS observations grouped per hour from set B for (a) Phoenix, AZ (KIWA); (b) Hastings, NE (KUEX); (c) Middleton Island, AK (PAIH); and (d) San Juan, PR (TJUA). Approximate sunrise (sunset) times are represented by the transparent vertical dashed (solid) bars for each location from the 4 months. All times are local standard time (LST). Different aspects of the diurnal cycles are described further in the text.

TABLE 4. Monthly mean of Z_{DR} bias estimates from CABS using continuous monitoring and the 2-h (1700–1900 UTC) window. A subset of these sites is plotted in Fig. 8. Empty spaces represent times when a site had no CABS detections for a month in a particular method. Overall, the difference in the mean values is within ±0.1 dB. Channel is abbreviated as Ch.

	Continuous monitoring				2 h (1700–1900)			
	Oct 2013	Jan 2014	Apr 2014	Jul 2014	Oct 2013	Jan 2014	Apr 2014	Jul 2014
KIWA mean	−0.05	−0.12	−0.06				0.00	
KOTX mean	−0.25	−0.29	−0.25	−0.19	−0.22	−0.31	−0.26	
KEYX mean	0.33	−0.80	0.11	0.17			0.06	
KUDX mean	−0.07	0.18	0.04		−0.09	0.28	−0.02	
KPUX mean	0.13	−0.35	−0.49		0.27	−0.40	−0.48	
KUEX mean	−0.03	−0.05	−0.07	−0.07	0.00	−0.04	−0.08	−0.06
KTLX mean	−0.53	−0.56	−0.25			−0.55	−0.25	
KILN mean	−0.48	−0.53	−0.54	−0.14	−0.45	−0.50	−0.52	−0.13
KJGX mean	−0.54	−0.46	−0.07	0.04	−0.53	−0.44	−0.13	
KGRR mean	0.14	0.16	0.21	0.23	0.15	0.11	0.21	0.21
KBHX mean	−0.19	−0.12	−0.07	−0.16		−0.09	−0.31	−0.16
KLCH mean	0.14	0.11	0.10	0.12		0.11	0.13	
KCBW mean	0.05	0.05	0.05	0.14	0.06	0.00	0.06	0.19
KLGX mean	0.09	−0.02			0.13	−0.06	−0.13	
PAIH Ch1 mean	−0.03	0.04	0.03	−0.01	−0.03	0.10	0.13	0.06
PAIH Ch2 mean		0.16				0.28		
PHMO Ch1 mean	0.11	0.01	0.03	0.14	0.03		0.02	0.19
PHMO Ch2 mean	−0.03	−0.04	−0.04	0.02	−0.09	−0.01	−0.14	−0.06
TJUA Ch1 mean	0.35	0.37	0.45	0.39				
TJUA Ch2 mean	0.25	0.35	0.38	0.34				

had only 14 sites barely exceed 8 days with estimates. Interestingly, not all of the sites in the top category are along the coast; even some of the interior sites gain estimates over most of the month. For this particular month, there are 2051 days (from all sites combined) with CABS estimates from continuous monitoring compared to only 531 days with the 2-h window. This almost fourfold increase in availability can benefit sites

by providing reliable updates to Z_{DR} bias on a more regular basis.

The convective environment of April limits set C to only 92% of sites due to VCP selection and/or precipitation contamination. For example, Salt Lake City, Utah (KMTX), never used an allowed VCP for the entire month. Despite the increasing biota and precipitation contamination commonly seen in April, many
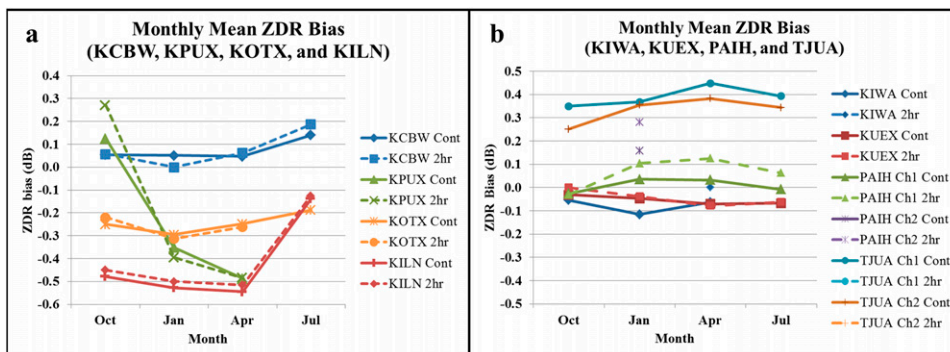

FIG. 8. Monthly mean of Z_{DR} bias estimates from the continuous monitoring (solid) and 2-h (1700–1900 UTC; dashed) CABS routine from the four focus months of the study. Two subsets of the 17-site set are shown (full set listed in Table 4): (a) Caribou, ME (KCBW); Pueblo, CO (KPUX); Spokane, WA (KOTX); and Cincinnati, OH (KILN); and (b) Phoenix, AZ (KIWA); Hastings, NE (KUEX); Middleton Island, AK (PAIH); and San Juan, PR (TJUA). PAIH used channel 1 for most of the year, resulting in a lack of channel 2 estimates, while TJUA has a distinct lack of CABS detections during the 2-h window (as seen in Fig. 7)—this results in no visible trace for those categories. When data are available, the differences between the methods are generally less than 0.1 dB.
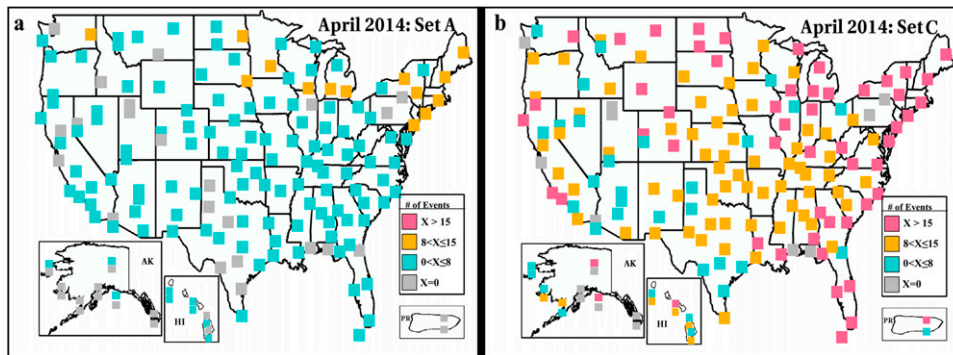
FIG. 9. Number of days with CABS estimates per site/channel using (a) the 2-h window compared to (b) continuous monitoring for April 2014. Color scale is the same as in Fig. 5. Continuous monitoring gives more days with at least one Z_{DR} bias estimate from CABS across the United States. Sites that do not have detections with continuous monitoring are mostly due to VCP constraints used in our algorithm.

sites—for example, sites in Texas—reported at least 3 times more days with CABS using continuous monitoring compared to the 2-h window. Although the statistical and precipitation filters were developed and refined for data from the 1700–1900 UTC time window and thus could be reducing availability from other times of day, the impact of these filters on limiting CABS estimation is likely smaller than using a nonallowed VCP across the WSR-88D fleet.

To visualize filter impacts on individual volume scan estimation, time series charts were generated for each site for the month of April 2014. These fields included the VCP in use, Z90th, interquartile range (IQR), filtered Z_{DR}, and filtered Z_{DR} with CABS (according to the 12-volume method used in our continuous monitoring routine). An example from TJUA (Fig. 10) will be used to describe some aspects of variability in more detail. The Z_{DR} modal estimates from CABS per volume scan (blue plus signs) show the high volume-by-volume variability that is greatly reduced by taking a 12-volume average (red circles). Note that a period with missing lines/points around 5 April 2014 reflects that TJUA was in a nonallowed VCP. From about 1200 UTC 10 April to 1200 UTC 15 April 2014, TJUA was using channel 2. It reveals how each channel can have a unique Z_{DR} bias, as the initial trend of about +0.45 dB appears to drop to about +0.25 dB with the channel change. The approximate times and general scatter for each channel have been highlighted for visual convenience.

Interestingly, the Z90th ≤ -3 dBZ threshold (described in detail in Part I) is rarely met at this site. A maritime environment may generally cause larger Z90th due to clouds and changing characteristics of isolated precipitation. The possibility also exists that the radar calibration of Z has a bias impacting the minimum detectable signal and thus the Z90th measurement. There

appears to be a diurnal variability to Z90th at TJUA that could relate to the almost daily isolated precipitation observed at many coastal sites or the diurnal bloom from biota and radar beam ducting (e.g., Hardy and Glover 1966; Schaefer 1976; Martin and Shapiro 2007). Times when Z90th is relatively high and IQR is relatively low suggest precipitation in the area (e.g., 17 April 2014). Meanwhile, times with high Z90th and high IQR suggest biota contamination associated with the diurnal bloom (e.g., 2 April 2014).

As expected, the variability of the volume-by-volume estimates appears very high in these charts. The TJUA channel 1 data suggest a range of about ± 0.25 dB, while the variability of the 12-volume averages is closer to ± 0.1 dB at this site. Such variability is likely return dependent. For example, a site with more contamination from ground clutter or biota (not shown) has higher volume-to-volume variability than seen at TJUA. For our study, the filters chosen work well for a majority of the sites throughout the year and reduce the overall chance of Z_{DR} bias estimation skewed by contamination.

4. Summary and discussion

An automated routine to estimate Z_{DR} bias from CABS, described in detail in Part I, was compared to other external target methods (light rain, dry snow) across the WSR-88D dual-polarization fleet. These external target methods sample mutually exclusive types of radar echo, each with specific filtering requirements and expected intrinsic values. Using CABS data minimizes the risk of using an incorrect intrinsic value, as ZDR$_{Intrinsic}$ from randomly oriented turbulent eddies is 0 dB. The trend of Z_{DR} bias over time, which is relatively stable without hardware failures or maintenance
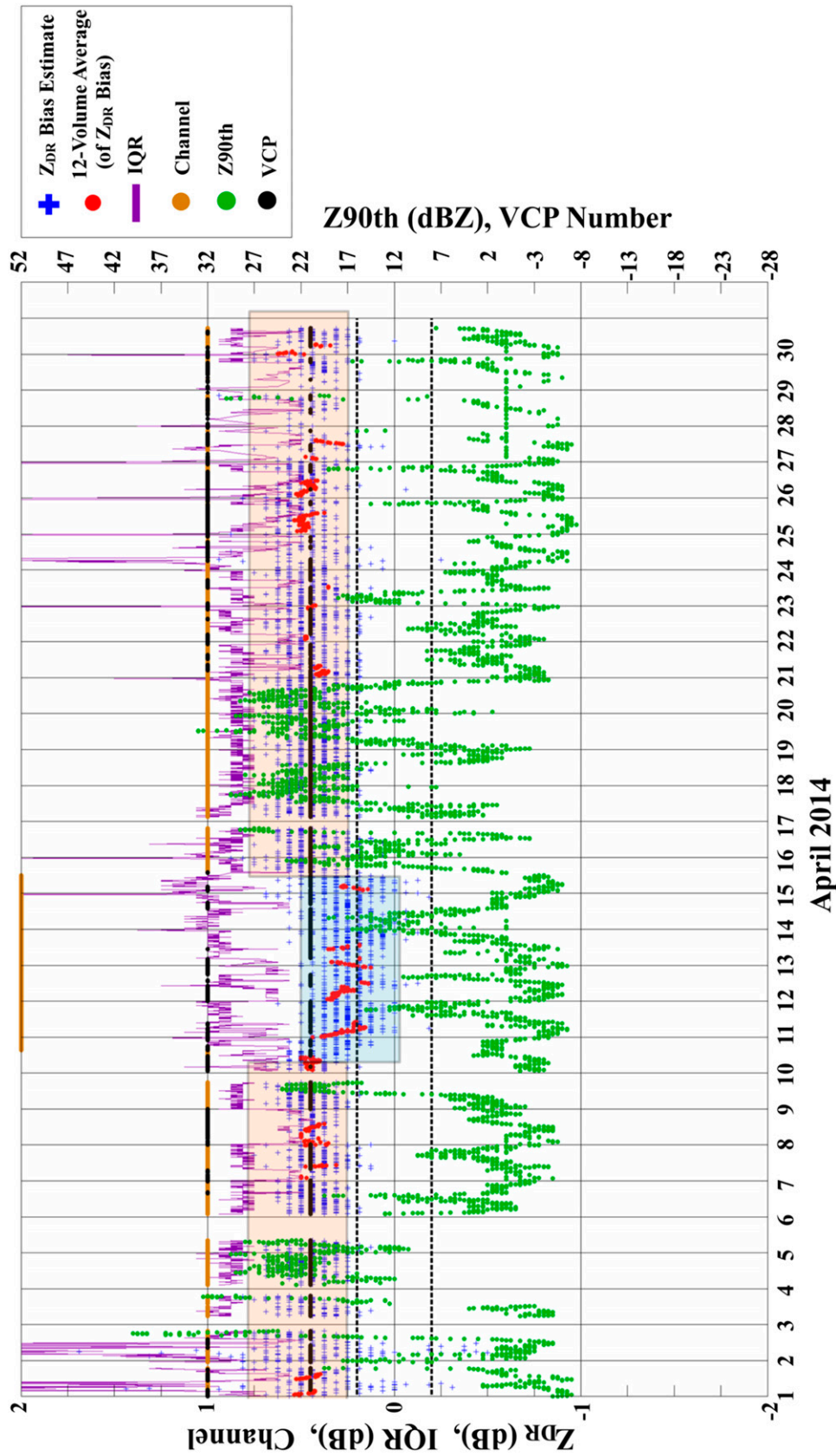
FIG. 10. Parameters from the continuous monitoring version of the CABS algorithm from San Juan, PR (TJUA), for each volume scan in April 2014. Estimates of Z_{DR} bias for channel 1 (channel 2) are highlighted in peach (blue)—the estimates in channel 2 are slightly lower than channel 1. More details and a discussion can be found in the text. The spurious linear trend of Z90th near the end of the month comes from "missing" points being set to 0.

actions, shows that CABS results compare well with the other external target methods (light rain and dry snow) based on shade charts.

The availability of CABS estimates seasonally and geographically was explored to discover potential limitations with this method throughout the year. CABS cases were more available in cool-season months because warm-season months have increased convective precipitation and biota contamination according to 1700–1900 UTC data from October 2013 through September 2014 across the United States. Results from the 2-h version appeared limited in certain geographic regions and during certain seasons. This unsurprising result highlights that CABS observed during 1700–1900 UTC is biased toward the midday heating in the central United States and does not capture optimal times of day for other climate regimes.

A modification to the original algorithm eliminated this time constraint and attempted to make a Z_{DR} bias estimate from CABS over the most recent 12-volume scans at any time (continuous monitoring). Because of the high variability of the volume-by-volume estimates of Z_{DR} modes, a 12-volume average was used as the Z_{DR} bias metric. Comparisons between the continuous monitoring and 2-h methods were measured in the number of days from a given month with at least one CABS estimate. On a site-by-site basis, the continuous monitoring of the CABS algorithm resulted in 2–4 times more days with estimates per month than the 1700–1900 UTC version. As such, it is recommended that the continuous monitoring version be used operationally and for future studies.

Monthly mean values of estimates were compared between the 2-h and continuous monitoring versions in terms of assessing long-term Z_{DR} bias at a site. Results were generally within ±0.1 dB of each other even with a large difference in the total number of estimates. This gave us confidence that the algorithm filters were effectively capturing data useful for Z_{DR} bias estimation. Thus, the time constraint could safely be removed with no modifications to the other filters.

Overall, an automated CABS routine can successfully provide Z_{DR} bias estimates throughout the year. This study is a first-look representation of the availability of Z_{DR} bias estimates from CABS detected by the WSR-88D and explores the temporal limitations of the automated algorithm in finer detail. Further research is needed to understand the full climatology of CABS and its use for Z_{DR} bias estimation or other areas of study, such as the depth of the convective boundary layer, turbulence intensity, gravity waves, and the intensity of convection. This method complements existing precipitation-based bias estimation techniques by providing estimates during clear weather and is not confined regionally or seasonally when widespread contaminants are not present. While future research is needed to define the variability and reliability of using any external target method for Z_{DR} bias estimation, similar results from three independent methods gives confidence in whether a bias exists at a site.

REFERENCES

Adams, D. K., and A. C. Comrie, 1997: The North American monsoon. *Bull. Amer. Meteor. Soc.*, **78**, 2197–2213, doi:10.1175/1520-0477(1997)078<2197:TNAM>2.0.CO;2.

Atlas, D., 1959: Meteorological "angel" echoes. *J. Meteor.*, **16**, 6–11, doi:10.1175/1520-0469(1959)016<0006:ME>2.0.CO;2.

Bechini, R., L. Baldini, R. Cremonini, and E. Gorgucci, 2008: Differential reflectivity calibration for operational radars. *J. Atmos. Oceanic Technol.*, **25**, 1542–1555, doi:10.1175/2008JTECHA1037.1.

Bringi, V. N., and V. Chandrasekar, 2001: Physically based parametric rain rate estimation algorithms. *Polarimetric Doppler Weather Radar: Principles and Applications*. Cambridge University Press, 636 pp.

Crum, T. D., R. L. Alberty, and D. W. Burgess, 1993: Recording, archiving, and using WSR-88D data. *Bull. Amer. Meteor. Soc.*, **74**, 645–653, doi:10.1175/1520-0477(1993)074<0645:RAAUWD>2.0.CO;2.

Cunningham, J. G., W. D. Zittel, R. R. Lee, and R. L. Ice, 2013: Methods for identifying systematic differential reflectivity (Zdr) biases on the operational WSR-88D network. *36th Conf. on Radar Meteorology*, Breckenridge, CO, Amer. Meteor. Soc., 9B.5. [Available online at https://ams.confex.com/ams/36Radar/webprogram/Paper228792.html.]

Davison, J. L., R. M. Rauber, and L. Di Girolamo, 2013a: A revised conceptual model of the tropical marine boundary layer. Part II: Detecting relative humidity layers using Bragg scattering from S-band radar. *J. Atmos. Sci.*, **70**, 3025–3046, doi:10.1175/JAS-D-12-0322.1.

——, ——, ——, and M. A. LeMone, 2013b: A revised conceptual model of the tropical marine boundary layer. Part III: Bragg scattering layer statistical properties. *J. Atmos. Sci.*, **70**, 3047–3062, doi:10.1175/JAS-D-12-0323.1.

Gorgucci, E., G. Scarchilli, and V. Chandrasekar, 1999: A procedure to calibrate multiparameter weather radar using properties of the rain medium. *IEEE Trans. Geosci. Remote Sens.*, **37**, 269–276, doi:10.1109/36.739161.

Hardy, K. R., and K. M. Glover, 1966: 24 hour history of radar angel activity at three wavelengths. *Proc. 12th Conf. on Radar Meteorology*, Norman, OK, Amer. Meteor. Soc., 264–268.

Ice, R. L., A. K. Heck, J. G. Cunningham, J. C. Hubbert, G. Meymaris, and M. Dixon, 2013: Polarimetric weather radar calibration—Engineering challenges. *36th Conf. on Radar*

Meteorology, Breckenridge, CO, Amer. Meteor. Soc., 9B4. [Available online at https://ams.confex.com/ams/36Radar/webprogram/Paper228789.html.]

——, ——, ——, and W. D. Zittel, 2014: Challenges of polarimetric weather radar calibration. Extended Abstracts, *Eighth European Conf. on Radar and Hydrometeorology (ERAD 2014)*, Garmisch-Partenkirchen, Germany, DWD and DLR, 8.1. [Available online at https://www.roc.noaa.gov/wsr88d/PublicDocs/Publications/Polarimetric_Calibration_Challenges_ERAD_2014_Ice_final_July18.pdf.]

Martin, W. J., and A. Shapiro, 2007: Discrimination of bird and insect radar echoes in clear air using high-resolution radars. *J. Atmos. Oceanic Technol.*, **24**, 1215–1230, doi:10.1175/JTECH2038.1.

Meischner, P. F., V. N. Bringi, M. Hagen, and H. Höller, 1991: Multiparameter radar characterization of a melting layer compared with in situ measurements. Preprints, *25th Int. Conf. on Radar Meteorology*, Paris, France, Amer. Meteor. Soc., 721–724.

Melnikov, V. M., R. J. Doviak, D. S. Zrnić, and D. J. Stensrud, 2011: Mapping Bragg scatter with a polarimetric WSR-88D. *J. Atmos. Oceanic Technol.*, **28**, 1273–1285, doi:10.1175/JTECH-D-10-05048.1.

——, D. Zrnić, M. Schmidt, and R. Murnan, 2013: Z_{DR} calibration issues in the WDR-88Ds: Report on 2013-MOU. NOAA, 54 pp. [Available online at http://www.nssl.noaa.gov/publications/wsr88d_reports/WSR88D_ZDRcalib_Report_2013.pdf.]

Ottersten, H., 1969: Atmospheric structure and radar backscattering in clear air. *Radio Sci.*, **4**, 1179–1193, doi:10.1029/RS004i012p01179.

Peel, M. C., B. L. Finlayson, and T. A. McMahon, 2007: Updated world map of the Köppen-Geiger climate classification. *Hydrol. Earth Syst. Sci.*, **11**, 1633–1644, doi:10.5194/hess-11-1633-2007.

Richardson, L. M., J. G. Cunningham, W. D. Zittel, R. B. Lee, R. L. Ice, V. M. Melnikov, N. P. Hoban, and J. G. Gebauer, 2017: Bragg scatter detection by the WSR-88D. Part I: Algorithm development. *J. Atmos. Oceanic Technol.*, **34**, 465–478, doi:10.1175/JTECH-D-16-0030.1.

Ryzhkov, A. V., S. E. Giangrande, V. M. Melnikov, and T. J. Schuur, 2005: Calibration issues of dual-polarization radar measurements. *J. Atmos. Oceanic Technol.*, **22**, 1138–1155, doi:10.1175/JTECH1772.1.

Schaefer, G. W., 1976: Radar observations of insect flight. *Insect Flight*, R. C. Rainey, Ed., Symposia of the Royal Entomological Society of London, Vol. 7, John Wiley & Sons, 157–197.

Schuur, T. J., A. V. Ryzhkov, and D. S. Zrnić, 2001: A statistical analysis of 2D-video-disdrometer data: Impact on polarimetric rainfall estimation. Preprints, *30th Int. Conf. on Radar Meteorology*, Munich, Germany, Amer. Meteor. Soc., 11B.4. [Available online at https://ams.confex.com/ams/30radar/techprogram/paper_21554.htm.]

——, ——, and D. R. Clabo, 2005: Climatological analysis of DSDs in Oklahoma as revealed by 2D-video disdrometer and polarimetric WSR-88D radar. *32nd Conf. on Radar Meteorology*, Albuquerque, NM, Amer. Meteor. Soc., 15R.4. [Available online at https://ams.confex.com/ams/32Rad11Meso/techprogram/paper_95995.htm.]

SPC, 2013: Severe weather climatology. Storm Prediction Center, accessed 23 June 2015. [Available online at http://www.spc.noaa.gov/new/SVRclimo/climo.php?parm=anySvr.]

Straka, J. M., D. S. Zrnić, and A. V. Ryzhkov, 2000: Bulk hydrometeor classification and quantification using polarimetric radar data: Synthesis of relations. *J. Appl. Meteor.*, **39**, 1341–1372, doi:10.1175/1520-0450(2000)039<1341:BHCAQU>2.0.CO;2.

Tauber, M. J., C. A. Tauber, and S. Masaki, 1986: *Seasonal Adaptation of Insects*. Oxford University Press, 411 pp.

Vivekanandan, J., V. N. Bringi, M. Hagen, and P. Meischner, 1994: Polarimetric radar studies of atmospheric ice particles. *IEEE Trans. Geosci. Remote Sens.*, **32**, 1–10, doi:10.1109/36.285183.

Zhang, G., J. Sun, and E. Brandes, 2006: Improving parameterization of rain microphysics with 607 disdrometer and radar observations. *J. Atmos. Sci.*, **63**, 1273–1290, doi:10.1175/JAS3680.1.

Zittel, W. D., J. G. Cunningham, R. R. Lee, L. M. Richardson, R. L. Ice, and V. M. Melnikov, 2014: Use of hydrometeors, Bragg scatter, and sun spikes to determine system Z_{DR} biases in the WSR-88D fleet. Extended Abstracts, *Eighth European Conf. on Radar in Meteorology and Hydrology (ERAD 2014)*, Garmisch-Partenkirchen, Germany, DWD and DLR, DAC. P12. [Available online at https://www.roc.noaa.gov/WSR88D/PublicDocs/Publications/132_Zittel.pdf.]

——, R. R. Lee, L. M. Richardson, J. G. Cunningham, J. A. Schultz, and R. L. Ice, 2015: Geographical and seasonal availability of light rain, dry snow, and Bragg scatter to estimate WSR-88D Z_{DR} system bias. *31st Conf. on Environmental Information Processing Technologies*, Phoenix, AZ, Amer. Meteor. Soc., 11.2. [Available online at https://ams.confex.com/ams/95Annual/webprogram/Paper265374.html.]